Temperature Dependence of Single-Asperity Diamond−Diamond Friction Elucidated Using AFM and MD Simulations

Matthew J. Brukman,[†,§] Guangtu Gao,[‡] Robert J. Nemanich,[†,||] and Judith A. Harrison*[,‡]

Physics Department, North Carolina State University, Raleigh, North Carolina 27695, Chemistry Department, United States Naval Academy, Annapolis, Maryland 21402, and Physics Department, Arizona State University, Tempe, Arizona 85287

Received: December 20, 2007; Revised Manuscript Received: March 21, 2008

Complementary experimental (atomic force microscopy) and theoretical (molecular dynamics) techniques were used to investigate friction between diamond−diamond junctions as a function of temperature. The simulation and experimental conditions were designed to correspond as closely as possible. In the atomic force microscopy (AFM) experiments, two microcrystalline-diamond (μCD) AFM tips of differing contact radii were used to examine the friction of diamond (111) and (001) single crystals from 24 to 225 K in an ultrahigh vacuum. At all temperatures, the experimentally determined dependence of friction on load was consistent with the occurrence of single-asperity interfacial friction, where friction is proportional to contact area. In addition, the behavior of the contact was fit well by the Derjaguin−Muller−Toporov continuum model. Friction measurements within a given series were highly repeatable; however, as is typical with AFM measurements, there was some variation in measurements taken from different regions of the sample and with different tips. Interfacial shear strength, or the intrinsic resistance to sliding, decreased slightly with increasing temperature for both surfaces. To shed additional insight into the AFM results, MD simulations were performed with the diamond single crystals of the same orientation. The calculations also show that the average friction force decreased slightly as the temperature increased for both diamond surfaces and for all sliding directions. Both AFM and MD results agree with the numerical analysis of friction as a function of temperature published by Sang et al. (Sang, Y.; Dube, M.; Grant, M. *Phys. Rev. Lett.* 2001, *87*, 174301).

Introduction

The diamond−diamond sliding interface is of interest to both the applied materials and research communities. Diamond is well-known for its hardness, chemical stability, and thermal conductivity.[1,2] These properties, coupled with its excellent friction and wear properties, make diamond potentially useful as a protective coating in a wide range of environments[3,4] and as a structural material for microelectromechanical (MEMS) and nanoelectromechanical (NEMS) systems.[5–9] An understanding of how diamond surfaces interact with each other under extreme temperature conditions is therefore valuable.

While the friction of diamond on the macroscopic level has been investigated extensively,[10–14] relatively few studies have examined the atomic-scale friction of diamond.[15–18] To date, the temperature dependence of the friction of diamond has not been examined using AFM (atomic force microscopy). Room temperature studies of the atomic-scale friction of diamond surfaces were performed using AFM with several types of tips and under different environmental conditions.[15–20] The nanoscale friction and contact area between a diamond (111)(1 × 1)-H surface and a tungsten carbide tip were measured in UHV (ultrahigh vacuum).[17,20] The current of the tip−sample contact as a function of load for that extremely hard heterocontact was shown to be described by the Derjaguin−Muller−Toporov (DMT)[21] model. The true contact area was extracted from the current data and shown to be directly proportional to the friction. This allowed for an interfacial shear strength, or intrinsic resistance to friction, of 238 MPa for the diamond−tungsten carbide interface to be determined.[17] Schwarz et al. also observed that friction was proportional to the area of contact between a hydrocarbon-coated tip and a microcrystalline diamond (μCD) in air and argon.[16]

The interfacial shear strength between spherical hydrocarbon-coated tips and diamond (001) and (111) was measured recently as a function of sliding direction in N_2 in a combined AFM-MD (molecular dynamics) study.[18] The AFM work revealed no difference in the interfacial shear strength for either surface in any sliding direction, and the reported values were in the range of 100−500 MPa. Earlier AFM experiments examined the friction between a CVD-grown diamond crystallite tip and single crystals of diamond (111) and (001) in UHV at room temperature. [15] Atomic-scale stick-slip was observed on both surfaces, and the scale of the friction forces between the tip and the surfaces was similar. Recent MD simulations that utilized the reactive empirical bond-order potential (REBO) also showed no statistically significant difference in friction between diamond (001) and diamond (111) at room temperature, except for the case of sliding at high pressures along the dimer row direction on the (001) surface.[18]

To date, few studies of the temperature dependence of single-asperity friction[22,23] or macroscopic friction[24,25] have been reported. Atomic-scale friction between a (native oxide-coated) silicon tip and a silicon (111) wafer (also with native oxide) was examined recently in UHV by AFM.[22] In that work, both the friction coefficient and the pull-off force between 50 and 300 K had a nonlinear dependence on temperature. In contrast,

* Corresponding author. E-mail: jah@usna.edu.
† North Carolina State University.
‡ United States Naval Academy.
§ Present address: Department of Materials Science and Engineering, University of Pennsylvania, Philadelphia, PA 19104.
|| Arizona State University.

10.1021/jp711959e CCC: $40.75
Published on Web 06/04/2008

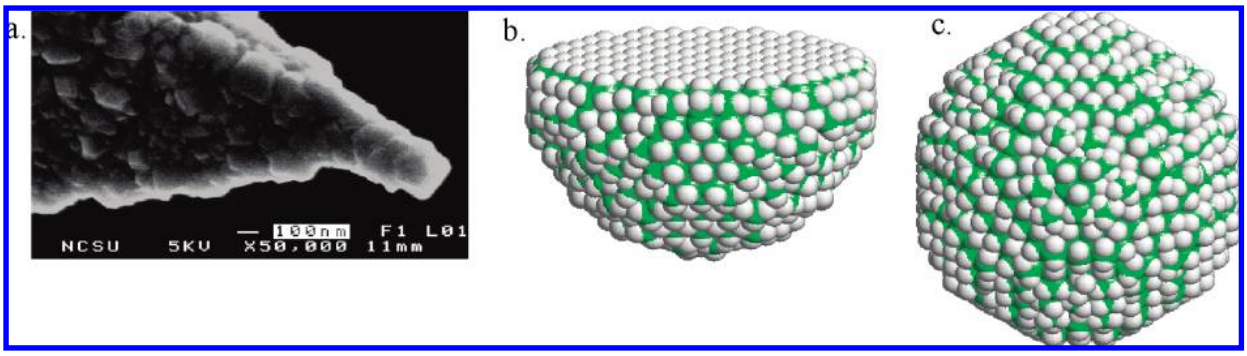

Figure 1. (a) SEM micrograph of μCD AFM after scanning (tip-2). (b) Curved-diamond tip used in MD simulations viewed from the side and (c) from the angle that contacts the diamond surfaces. Large green and small white spheres represent carbon and hydrogen atoms, respectively.

the friction force was reported as varying linearly with load for all temperatures with the low-temperature and high-temperature data having different slopes. These data were not fit to continuum mechanics models, and therefore, the shear strength of the interface was not reported. The AFM also has been used to examine the friction between a silicon nitride tip and highly oriented pyrolytic graphite (HOPG) from 140 to 800 K.[23] The friction force had a linear dependence on load and, in contrast to the SiO_2-SiO_2 interface, it decreased exponentially with increasing temperature between 140 and 280 K. The friction force was below the detectable limit between 280 and 800 K.

Different trends were observed in the previous variable temperature (VT) studies of atomic-scale friction force and friction coefficient with temperature. Because the materials in sliding contact were different in both studies, similarities in observed trends are not expected a priori. There are many examples in the literature where joint AFM-MD studies were successfully utilized to examine processes at very small length scales.[18,26–28] With that in mind, complementary state-of-the-art AFM and MD studies aimed at determining the dependence of friction on temperature between well-characterized, ideally hard diamond tip−diamond surface contacts were performed. The MD simulations examined the friction between a curved, finite-sized diamond tip and hydrogen-terminated diamond (001) and (111). The AFM experiments used μCD tips to examine the friction of those same diamond surfaces, while the simulations provide insight into the atomic-scale origins of the observed behavior. Because some significant differences between experiments and simulations do exist, the limitations imposed by these differences also are discussed.

Methodology

Complementary AFM experiments and MD simulations of nanoscale friction as a function of temperature for (111) and (001) single-crystal diamonds were performed. In AFM, forces at the sliding junction were detected by a tip at the end of a compliant cantilever beam that bends out-of-plane in response to a normal force and twists as shear forces impart a torque to the tip.[29] The bending and twisting were sensed using an optical beam and a four-quadrant photosensitive detector. Friction force was taken to be half the difference between the average of lateral force trace and retrace signals over the middle third of each scan line.[30]

Quantitative information can only be obtained from AFM measurements by using carefully calibrated cantilevers.[31–33] Cantilevers were individually calibrated in the normal force by the vendor. While the actual cantilevers used for scanning could not be directly calibrated, many levers from the same batch were independently calibrated using the Sader et al. method[33] and were within the specifications reported by the vendor ($\pm$10%). The wedge lateral force calibration technique was performed on all cantilevers using Mikromasch TGG01 grating.[34] The Omicron system does not allow lateral adjustment of the photodetector, which results in a decrease in sensitivity. This loss of sensitivity (i.e., signal-to-noise) increases the error associated with the lateral calibration. Finally, a cantilever tilt compensation was employed to negate the local topography of the diamond surfaces.[35]

Varying the normal load smoothly over a single image necessitated an additional circuit in the AFM feedback loop.[36] Within each image, the normal force decreased from high (compressive) to low (tensile) load until the tip pulled off the sample, allowing the determination of adhesive (pull-off) forces. Scans were performed at 2 Hz with scan lengths of 25 nm for tip-1 and 40 nm for tip-2. Thus, the scanning speeds were 100 and 160 nm/s for tip-1 and tip-2, respectively. Because samples could not be rotated in situ, friction on each surface was examined in one direction on each surface: the [010] direction on the (001) surface and the $[11\bar{2}]$ direction for the (111) surface. Polished commercial diamond (111) (Delaware Diamond Knives) and diamond (001) (Sumitomo Carbide) were used for friction measurements. To avoid roughening the surfaces, no attempt to achieve complete hydrogen termination of the diamond surfaces was made. The specimens were cleaned by sonication in acetone and methanol, rinsed with deionized water, and jet-dried with N_2. In situ Auger analysis indicated that the surfaces were free of contamination and that the (111) and (001) surfaces contained 0.16 and 0.21 monolayers of oxygen, respectively. Unfortunately, the way in which oxygen is bound to the surfaces remains an open question. Recent ab initio studies on the diamond (001) surface showed that in the presence of hydrogen, oxygen will be in the form of -OH.[37]

Two μCD diamond-coated AFM tips were used (Nanosensors DT-CONTR) (Figure 1). Examination of the sharpness of the wedge crests during calibration allowed for the determination of the radii of both tips (30 ± 5 and 60 ± 5 nm for tip-1 and tip-2, respectively) after friction measurements.

The VT-AFM cryostat uses blowoff from liquid helium to lower the temperature of a cooling block in contact with the sample holder. The diamond crystals were fastened to the sample holder via silver-based epoxy and molybdenum foil. Thermocouples measured the temperatures of the cryostat to be 4 K, while the cooling block reached temperatures as low as 24 K. Thermal losses in the system were accounted for, and sample temperatures were determined from the measured cooling block temperatures according to calibration data provided by the

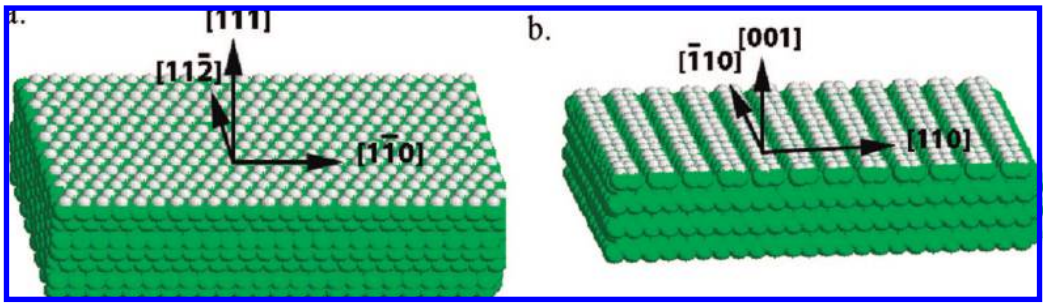

Figure 2. Schematic representation of diamond surfaces examined here: hydrogen-terminated diamond (111)(1 × 1) and (001)(2 × 1) surfaces in panels a and b, respectively. Large and small spheres represent carbon and hydrogen atoms, respectively.

manufacturer. The measurements were taken from low to high, and the sample stage temperatures were 48, 91, 135, 180, and 225 K.

The MD simulations utilized a curved-diamond tip that was constructed from a diamond (111) crystal by removing atoms to make a roughly hemispherical tip with a radius of 15 Å (Figure 1). The surface atoms were saturated by adding hydrogen atoms, and the tip contained 1352 sp^3-bonded carbon and 520 hydrogen atoms. Knowledge of the forces on the cantilever and the shape of the AFM tip (i.e., the geometry of the contact zone) is crucial for extracting quantitative data from AFM experiments. This tip was designed to model the shape of a typical AFM tip. However, computational power limits our ability to simulate a tip of the same size as those in the experiment. The effects of tip shape on the simulated results have been examined previously.[18] In that work, the friction between nanowire tip with a flat contacting surface and single-crystal diamonds was examined. While the shapes of the friction versus load curves at 300 K obtained with both tips varied somewhat, the qualitative conclusions reached when using both tips were the same. Consequently, we only report results for friction as a function of temperature for the curved tip in this work. The curved tip was stepped and incommensurate with both of the diamond surfaces in all sliding directions, and it was used to examine the friction of diamond (111)(1 × 1)-H and (001)(2 × 1)-H as a function of temperature at several loads.

The (111) and (001) samples both have 13 layers of carbon (Figure 2). For each sliding simulation, the sample was made slightly wider in the sliding direction. Table 1 summarizes the total number of atoms in each sample, the dimensions, and the sliding directions. The samples were partitioned into three regions. The atoms in the farthest layer from the interface, in the middle region, and closest to the sliding interface were held fixed, had a thermostat applied to maintain the temperature,[38] and were unconstrained, respectively. The time step for all simulations was 0.25 fs. To simulate a system under constant external load, an external force was applied to the tip in the direction perpendicular to the diamond sample, and the entire tip was treated as a rigid body.

Dimensions of the diamond substrates were selected to be as large as possible, while remaining computationally feasible. To simulate an infinite sliding surface, periodic boundary conditions were applied in the plane that contained the surfaces. The tip dimensions were such that it did not interact with its periodic image. Because many simulations are required, the total number of atoms in the simulation must be considered when selecting the simulation size. Indeed, the MD tips are an order of magnitude smaller than the AFM tips, and the MD sliding speeds are 7 orders of magnitude greater than the AFM speeds. These are universal issues for most state-of-the-art MD and AFM measurements. Because the sliding speeds are below the sound speed of diamond in the MD simulations, dynamical effects due to the resonant inducement of sound waves are not expected.

The tip is brought into contact with the surfaces by placing it above the diamond surfaces at a distance where the potential energy equals zero and then moving it at a constant speed of 1.0 m/s toward the diamond surfaces. Sliding simulations were performed by moving with a constant external load applied to the tip while it moves parallel to the diamond substrate at a constant speed. Tip speeds of 0.84 and 1.0 m/s both were used. As the tip slides, the friction force oscillates in periodic cycles about a constant value. Tip speeds were chosen so that the friction force experiences an integer number of complete oscillation cycles within each unit cell. Governed by dynamic equations from Newton's laws, the tip will oscillate around an average height relative to the film, resulting in an average load on the film equal to the constant force on the tip.

The second-generation REBO potential,[39,40] which was parametrized to model solid- and gas-phase hydrocarbon systems and is capable of modeling chemical reactions, was used. The second-generation REBO, and its predecessor,[41] were used to model the mechanical properties of filled[42] and unfilled nanotubes,[43] the properties of clusters,[44] the adhesion and tribochemistry of diamond surfaces[45–47] with and without chemically bound hydrocarbon chains,[48,49] the friction and wear of amorphous carbon films,[50,51] and the stress at grain boundaries.[52,53] Recently, the second-generation REBO potential was shown to accurately reproduce the 0 K elastic constants of diamond and graphite and to qualitatively reproduce the trends in elastic constants of diamond as a function of temperature.[54,55]

The adaptive intermolecular REBO (AIREBO) potential is an extension of the second-generation REBO potential that includes intermolecular van der Waals forces.[56] Simulations conducted with AIREBO are approximately 7 times slower than those carried out with the REBO potential. A small number of simulations was carried out using both the AIREBO and the REBO potentials. While the qualitative trends in the average friction obtained with both potentials are the same, the error bars associated with the average friction are noticeably smaller when the AIREBO potential is used. The magnitude of the fluctuations in the Lennard-Jones forces at the interface is smaller than the fluctuations in the covalent forces.[57] As a result, the error bars are smaller when the AIREBO potential is used. Because the qualitative trends are the same, and the computational time required for simulations with the REBO potential is significantly less, the REBO potential was used for the simulations presented here. Results for a small number of simulations conducted using the AIREBO potential also are discussed. Previous examinations of the atomic-scale friction of a tungsten−carbon diamond interface have shown that the contact area as a function of load (and the friction vs load) can be

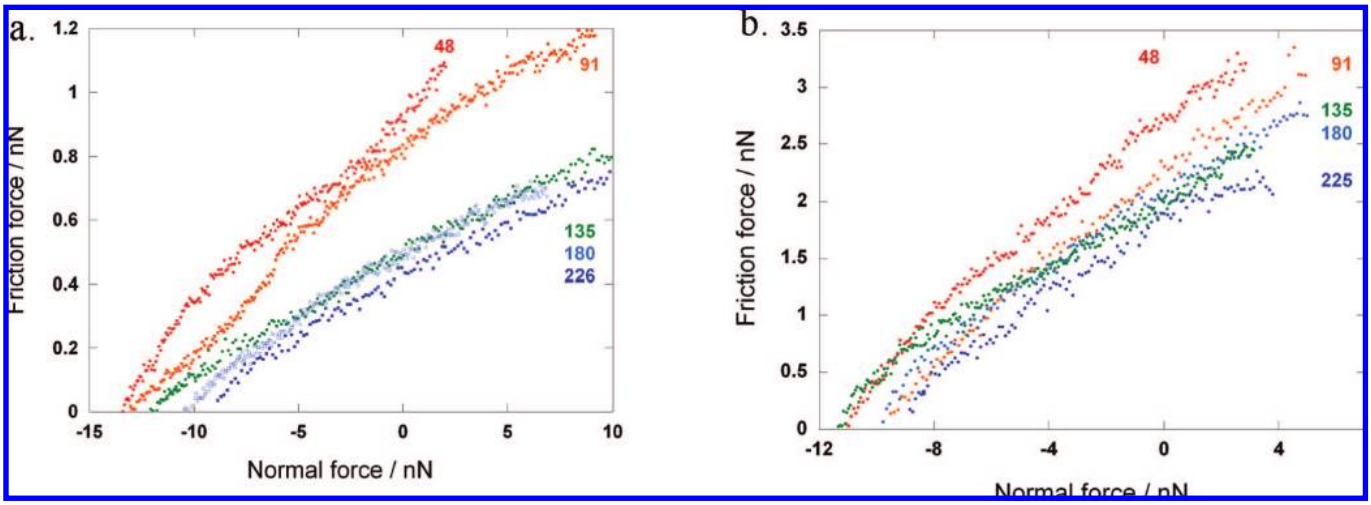

Figure 3. Average of friction vs load data sets at several temperatures taken with the same AFM tip (tip-1). Panels a and b show the (001) and (111) surfaces, respectively. COS transition fits were performed on these data, the work of adhesion (γ), transition parameter (α), and shear strength of the interface obtained are shown in Table 2 and Figures 5 and 6.

TABLE 1: Details of Surfaces and Sliding Directions Used in MD Simulations

		MD parameters				
surface	sliding direction	no. of C atoms	no. of H atoms	*X* size (Å)	*Y* size (Å)	*Z* size (Å)
(111) (1 × 1)-H	[1$\bar{1}$0]	4992	384	60.5	34.9	13.35
(111) (1 × 1)-H	[11$\bar{2}$]	5096	392	35.3	61.1	13.35
(001) (2 × 1)-H	[1$\bar{1}$0]	5096	392	35.3	70.6	11.75
(001) (2 × 1)-H	[110]	4368	336	60.5	35.3	11.75

described by the DMT contact mechanics model.[17,20] This is also true of the AFM data reported here. Therefore, despite the absence of adhesion in the MD simulations, the DMT limit is a valid approximation for simulations because an adhesion term simply shifts the load by the pull-off force.

Unless otherwise indicated, the reported friction forces were obtained by averaging data from two sliding simulations with independent starting configurations. These two configurations were obtained by translating the tip a fraction of a unit cell distance in the direction perpendicular to the sliding direction. For each individual simulation, the instantaneous friction force (force in the sliding direction) on the tip was recorded every 1 fs. The sliding distance was divided into unit cell segments (based on the diamond surface), and the instantaneous forces were averaged over these unit cell segments. The values for each unit cell segment were then averaged to obtain an average friction force for a given simulation at each load. Because the contact area is small and the fluctuations in the forces are large, the error bars are large.[57] In a typical AFM measurement, either by design or by imperfect tilt compensation, scan lines will not overlap each other perfectly. Thus, averaging over different starting configurations approximates the experimental line-averaged response.

Results

Experimental Measurements. While independent verification of the validity of continuum mechanics models at the nanometer scale is still lacking, these models have been routinely used to interpret the frictional behavior of nanometer-sized contacts. The DMT and Johnson−Kendall−Roberts[58] (JKR) continuum contact models, which represent a limiting case of adhesive, sphere-on-flat contact behavior, have been widely used to interpret AFM data. The JKR model is valid when the contacting surfaces are compliant and attractive forces are strong, short-ranged, and significant only when the materials are in contact. The DMT model describes contact behavior at the other end of the spectrum when the materials are stiff, the sphere radii are small, and the attractive forces are weak and long-ranged. For example, the contact current as a function of load between tungsten carbide tip and diamond (111)(1 × 1)-H in UHV was recently shown to be fit by the DMT model.[17,20] Because the friction was proportional to the load, the friction versus load data also could be fit by the DMT model. Nonidealized contacts fall between JKR and DMT limits and may be analyzed using transition models, such as Maugis-Dugdale,[59] or transition fits, such as the method proposed by Carpick, Ogletree, and Salmeron (COS).[34] Recently, the COS analysis method was used successfully to analyze friction versus load data that result when a hydrocarbon tip is in sliding contact with diamond (001)(2 × 1)-H and (111)(1 × 1)-H oriented grains on μCD.[18] The COS formulation also recently was derived analytically by Schwarz.[60]

Representative friction versus load data (FL) obtained for each diamond surface with tip-1 at several temperatures are shown in Figure 3. (Corresponding curves from tip-2 are qualitatively similar and are not shown.) Several trends are apparent in these data. First, on both surfaces, the magnitude of the friction force is smaller at higher temperatures. Second, while the pull-off forces on both surfaces are comparable, the magnitude of the friction force is larger on the (111) surface. The magnitude of the measured friction force is influenced by surface inhomogeneities. These include surface chemical or structural defects such as dangling bonds, C−O moieties (which are present on both surfaces), -OH moieties, and vacancies. The quantity that is most influenced by these inhomogeneities is the pull-off (adhesive) force.[61]

The pull-off forces for both diamond surfaces are shown as a function of temperature in Figure 4 for both AFM tips. When tip-1 is used, adhesion forces for the (001) and (111) surfaces are comparable. When the larger tip (tip-2) is used, the pull-off

TABLE 2: Summary of Material and Interfacial Properties for Diamond−Diamond Contact in UHV[a]

surface, direction	temp (K)	γ (mJ m^{-2}) ± 22%	τ_0 (MPa) ± 25%	zero-load friction (nN) ± 25%	$\tilde{C}$ (N$^{1/3}$ m$^{-2/3}$) ± 24%	λ
tip-1, R = 30 nm	50	64	430	0.84	16	20×10^{-3}
	90	62	390	0.73	15	20×10^{-3}
(111), [11$\bar{2}$]	135	87	410	0.97	15	10×10^{-3}
	180	53	370	0.62	30	10×10^{-3}
	225	49	370	0.60	14	3×10^{-3}
	50	72	410	0.91	17	40×10^{-9}
(001), [010]	90	70	370	0.81	15	10×10^{-3}
	135	60	290	0.56	12	80×10^{-9}
	180	53	290	0.52	12	80×10^{-9}
	225	46	280	0.45	11	1×10^{-3}
tip-2, R = 60 nm	50	122	600	4.7	23	8×10^{-3}
	90	120	710	5.5	27	40×10^{-3}
(111), [11$\bar{2}$]	135	112	630	4.2	34	2×10^{-3}
	180	109	560	4.5	21	20×10^{-3}
	225	66	340	1.8	13	5×10^{-3}
	50	42	520	2.1	21	7×10^{-3}
(001), [010]	90	64	420	2.2	17	10×10^{-3}
	135	85	450	2.9	18	50×10^{-3}
	180	75	400	2.6	16	20×10^{-3}
	225	50	330	1.6	13	90×10^{-3}

[a] Uncertainties are a combination of standard error (<5%) and uncertainty in physical constants (calibration factors, tip radius, and elastic constants).

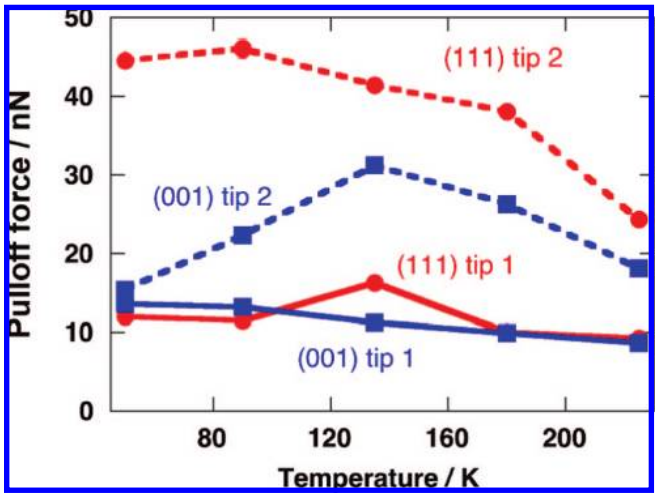

Figure 4. Pull-off force as a function of temperature from AFM experiments. Error bars are standard errors and represent variation within a set of measurements for a given tip−sample pair at a given temperature (N > 15). Error bars are approximately the size of the points.

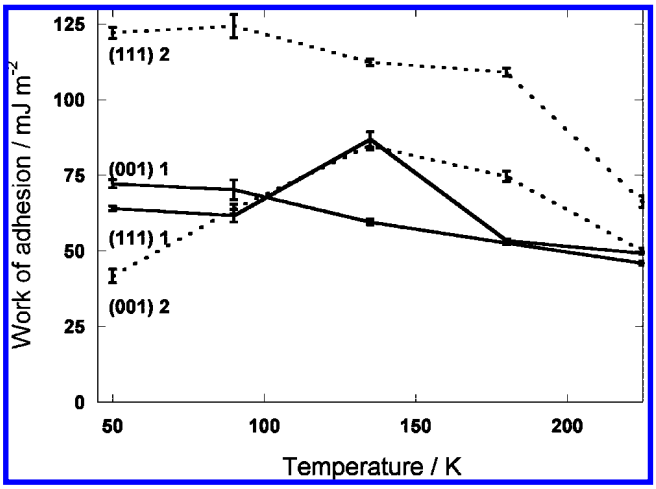

Figure 5. Work of adhesion at several temperatures calculated from COS fits to friction vs load AFM data. Error bars are standard errors and represent variation within a set of measurements for a given tip−sample pair at a given temperature (N > 15). Data sets using two different AFM tips are shown (designated as 1 and 2).

forces are approximately twice as large on both surfaces, and the friction forces are greater as well. This analysis of adhesion is complicated by the fact that data taken with tip-1 and tip-2 were measured on different regions of a given diamond crystal. Thus, the local surface chemistry in each region could differ. The variation in data sets is a persistent problem in AFM that has yet to be rigorously addressed in the literature. These difficulties are exacerbated when the additional variable of temperature is introduced.

Despite the limitations of continuum mechanics at this scale, agreement between measurements and predicted functional form of friction versus load data has been found.[20,62–65] While many experimental variables can influence the quantitative numbers obtained from the fits, certainly a comparison of these numbers remains valid as long as the experimental conditions are precisely defined. An additional benefit to performing these fits is that the interfacial shear strength of the interface, τ_0, which should not be influenced by the pull-off force, can be obtained. With these things in mind, the friction versus load data have been fit to a continuum mechanics model using the COS transition method.[34]

The COS transition scheme determines the transition parameter λ from AFM friction versus load data. Values of λ greater than 5 correspond to the JKR model of contact mechanics, while values below 0.1 correspond to the DMT model. In this work, the median value of λ for each tip−sample combination was <0.1 (Table 2). Thus, the μCD−single-crystal diamond interface generally exhibited DMT contact mechanics. Friction forces at junctions of this type are proportional to the true contact area or $F_f = \tau_0 A$.[20]

The effective shear strength $\tilde{C}$ of the interface is related to τ_0 according to $\tilde{C} = \pi\tau_0 K^{-2/3}$, where K is the reduced elastic modulus of the contact given by $K = 4/3(\{1 - \nu_{surf}^2\}/E_{surf} + \{1 - \nu_{tip}^2\}/E_{tip})^{-1}$, where the Young's moduli of the surface and the tip are E_{surf} and E_{tip}, and ν_{surf} and ν_{tip} are Poisson's ratios for surface and tip, respectively. The effective shear strength is a useful metric tool when the material properties of the two contacting materials are not known and has been used

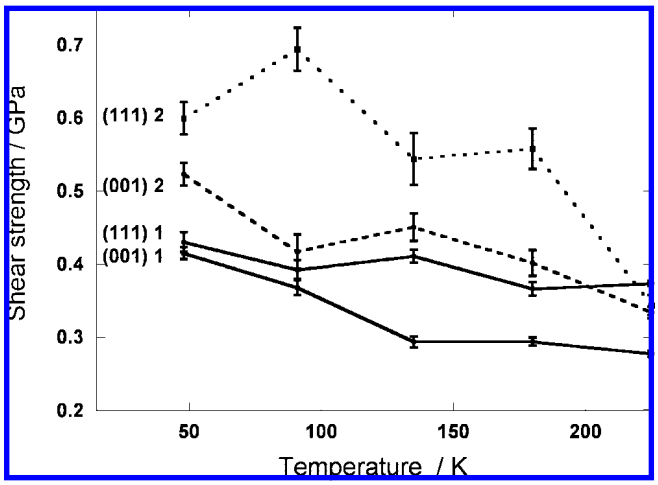

Figure 6. Interfacial shear strengths for diamond−diamond contact calculated from COS fits to the friction vs load AFM data. Error bars are standard errors and represent variation within a set of measurements for a given tip−sample pair at a given temperature ($N > 15$). Data sets using two different AFM tips are shown (designated as 1 and 2).

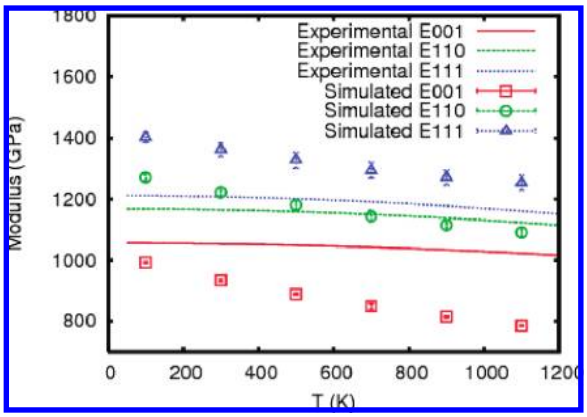

Figure 7. Young's moduli as a function of temperature for three crystal faces of diamond calculated from MD simulations. Experimental data are also shown for comparison.[67]

by several groups.[16,18] The material properties of diamond have been studied extensively, and it is possible to calculate Young's modulus and Poisson's ratio as a function of temperature for each diamond surface using the equations published by Turley and Sines.[66] This allows for the calculation of interfacial shear strength. The work of adhesion γ is also obtained from the COS fits and is given by $\gamma = \gamma_1 + \gamma_2 + \gamma_{12}$, where γ_1 and γ_2 are the surface energies of each contacting surface and γ_{12} is the interfacial free energy.

The work of adhesion and interfacial shear strength is shown as a function of temperature in Figures 5 and 6 (and Table 2), respectively. While the tip-1 and tip-2 data were taken on different regions of the crystals and are subject to some variability, analysis of data in Figures 5 and 6 reveals some interesting trends. For both crystal surfaces, the work of adhesion values falls between 40 and 120 mJ/m^2 over the entire temperature range, and γ generally decreases slightly with increasing temperature, although there is scatter in these data. The values of τ_0 obtained with both tips also decrease slightly with increasing temperature. With the exception of data obtained with tip-2 on the (111) surface, the values of τ_0 obtained for both crystals at each temperature are generally comparable.

MD Simulations. To extract the interfacial shear strength from AFM friction versus load data, the reduced modulus of the system must be known. The value of K is a function of temperature because it contains Young's moduli and Poisson ratios of both tip and substrate, which are all temperature-dependent. Thus, if MD results are to be compared to AFM data, the simulations should do an adequate job reproducing qualitative trends in the elastic properties of the materials under consideration as a function of temperature.

Young's moduli are shown in Figure 7 as functions of temperature. The simulated values were calculated using the formulae given by Turley and Sines,[66] and the elastic constants were calculated as a function of temperature using the second-generation REBO potential.[54] For all temperatures examined, $E(111) > E(110) > E(001)$, a trend that is in agreement with experimentally determined data.[67] In addition, both experimentally determined and calculated values of Young's moduli decrease with increasing temperature. However, the calculated values decrease more markedly with temperature than the experimental values. This fast softening of the moduli is a consequence of the elastic constants decreasing too markedly with increasing temperature, which, in turn, is a result of a large thermal expansion coefficient obtained from classical MD simulations. Gruneisen's Law states that larger thermal expansion coefficients result in faster elastic softening.[68] The failure to reproduce the correct thermal expansion coefficients is a known shortcoming of classical MD below the Debye temperature and can only be corrected with the inclusion of quantum mechanical effects.

The atomic-scale friction between hydrogen-terminated curved tip and diamond (111)(1 × 1)-H and diamond (001)(2 × 1)-H was investigated using MD simulations. The average friction as a function of temperature is shown in Figure 8. For each surface, two perpendicular sliding directions and two external loads were examined. In all cases, the average friction decreases slightly as the temperature is increased. Despite the large error bars associated with average friction, a detailed examination of these data reveals some interesting trends. First, for data obtained at a load of 60 nN, the friction force on the (001) surface for each sliding direction is statistically different at all temperatures. In other words, the error bars do not overlap. The friction on the (111) surface is statistically equivalent for both sliding directions only at the highest two temperatures. Lastly, at 300 K, the error bars associated with friction of both (001) and (111) surfaces overlap at both loads. Thus, the friction is statistically equivalent at this temperature, with the exception of the $[\bar{1}10]$ direction on the (001) surface. This trend was reported in our earlier simulations and is due, in part, to the large error bars associated with the average friction.[18] If the size of the error bar associated with the friction could be reduced so that the error bars do not overlap, the friction when sliding in different directions on the (111) surface would differ. In the data reported here, the size of the fluctuations in the instantaneous forces on the tip results in large error bars. Averaging over additional starting configurations is unlikely to have a marked influence on the size of the error bar because the force fluctuations remain large. Reducing the size of the force fluctuations could be accomplished by increasing the size of the tip (more atoms in contact) or by reducing the strength of the interactions at the tip−sample interface. [57] The latter can be accomplished by using the AIREBO potential. [56]

Because of limited computational resources, the average friction data for the 100 nN load were obtained from one sliding simulation with the friction averaged over unit cell segments (Figure 8). As was the case at the lower load, the average friction for all the surfaces and all sliding directions decreased slightly with increasing temperature. It is interesting to note that the

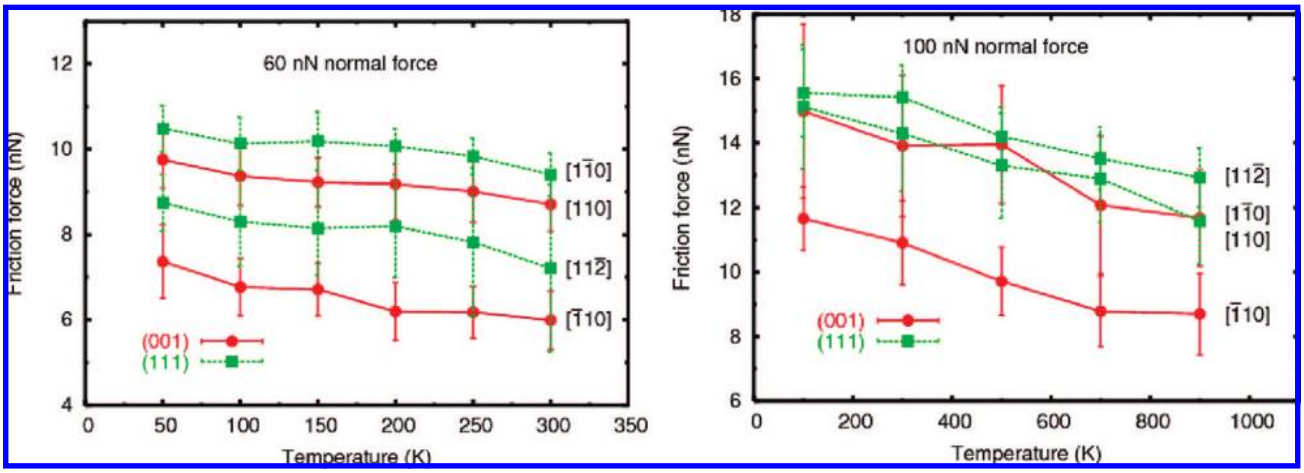

Figure 8. Average friction force (points) as a function of temperature for the (001) (red) and (111) (green) surfaces. Sliding directions and loads are given in the legends. Points represent the friction averaged over the diamond unit cell in the sliding direction. The error bars correspond to 1 standard deviation. When two sliding simulations were performed at each load, the average friction and the error bars at each load were averaged. Points are connected to aid the eye.

application of the additional load caused the average friction values (points in Figure 8) for the (111) surface in each sliding direction to be much closer to one another, while the friction for the (001) surface in each sliding direction was still separated by approximately the same amount.

Some insight into the magnitude of the average friction forces generated in the MD simulations (Figure 8) can be gleaned from the potential energy contours shown in Figure 9. These contour diagrams were generated by rastering the curved tip over the diamond surfaces at a fixed height and calculating the potential energy of the system. In the case of the (001) surface, sliding in the [110] direction corresponds to a larger value of average friction than when sliding in the [$\bar{1}$10] direction at both loads. This direction corresponds to sliding parallel to the surface dimer bond. Examination of the potential energy contour for the (001) surface reveals that when sliding in this direction, the hydrogen atoms are not equivalent. Sliding in this direction causes the tip to encounter a C−H bond tilted in the sliding direction and one tilted away from the sliding direction. In contrast, sliding in the [$\bar{1}$10] direction corresponds to sliding perpendicular to the dimer bonds. When sliding in this direction, the C−H bonds are canted in the same way and are therefore equivalent. Examination of the average friction data and the contour diagrams for both surfaces reveals that at 60 nN load, the sliding direction with the smallest repeat distance has the largest friction. As a result, the tip encounters more surface atoms and dissipates more energy. The average kinetic friction is the largest on the (111) surface in the [1$\bar{1}$0] direction and smallest on the (001) surface in the [$\bar{1}$10] direction, or $F_{[1\bar{1}0]}(111) > F_{[\bar{1}10]}(001)$. Examination of the density of surface atoms σ on these crystal faces of diamond reveals that the same trend in friction is apparent in the density of surface atoms, or σ (111) > σ (001).

To calculate the shear stress at the interface during sliding from the MD simulations, the contact area between the curved-diamond tip and the diamond substrates must be known. The contact force on a substrate atom is the force it experiences due to only the tip atoms. The hydrogen atoms on the surface of the diamond substrates sustain the majority of these forces, while the subsurface carbon atoms experience relatively small forces. The method of Luan and Robbins[63,64] can then be used to convert the number of surface atoms with a nonzero normal force to a contact area by taking the ratio of surface atoms in contact to the total number of atoms and multiplying by the total surface area. Once the contact area is known, it can also be used to calculate the normal pressure within the contact.

Previous MD simulations that have examined the static and kinetic friction of adsorbed monolayers have found that the average yield stress is related to the local pressure P within the contact via the equation $\tau_s = \tau_a + \alpha P$,[69,70] where α is a parameter that depends on the chemical constituents of the two surfaces but not on parameters that are not controlled in the experiments. In this equation, τ_a represents the adhesive contribution to friction because it is the yield stress when P is equal to zero. Previous work has shown that τ_a is approximately proportional to temperature, decreasing as the temperature increases, and that α has a weak dependence on temperature.

The static friction between the (111) surface and the curved tip at 300 K was calculated for sliding in the [1$\bar{1}$0] direction. The static friction depends linearly on P. The value of τ_a obtained from these data is negative, as expected when the interactions are purely repulsive.[69]

The kinetic friction data also can be fit to an equation of the form $\tau_s = \tau_a + \alpha P$. The shear stress as a function of the normal pressure for the (111) surface at three different temperatures when sliding in the [1$\bar{1}$0] direction is shown in Figure 10. In this case, the shear strength is defined as the average kinetic friction divided by the contact area ($\langle F_k \rangle / A$), and the normal pressure is defined as ($\langle F_N \rangle / A$). Because α should have a weak dependence on temperature, an average value of α was used for the three sets of data, and a value of τ_a was determined using a least-squares fitting procedure. (The average value of α was determined from a least-squares fit to the kinetic friction data and using τ_a obtained from the static friction data at each temperature.) The data shown in Figure 10 are linear, and the slope of the lines are in the range of 0.154, which is comparable to values obtained in previous MD simulations.[69,70] The values of τ_a obtained from these fits decrease with increasing temperature as expected. The values of τ_a at 300, 500, and 700 K are -0.115 ± 0.21, -0.421 ± 0.21, and -0.870 ± 0.19 GPa, respectively.

Discussion

Continuum mechanics models have been used successfully to interpret the frictional behavior of contacts on the nanometer scale, but the applicability of these models at the nanoscale is still a matter of debate. Recent MD simulations have shown

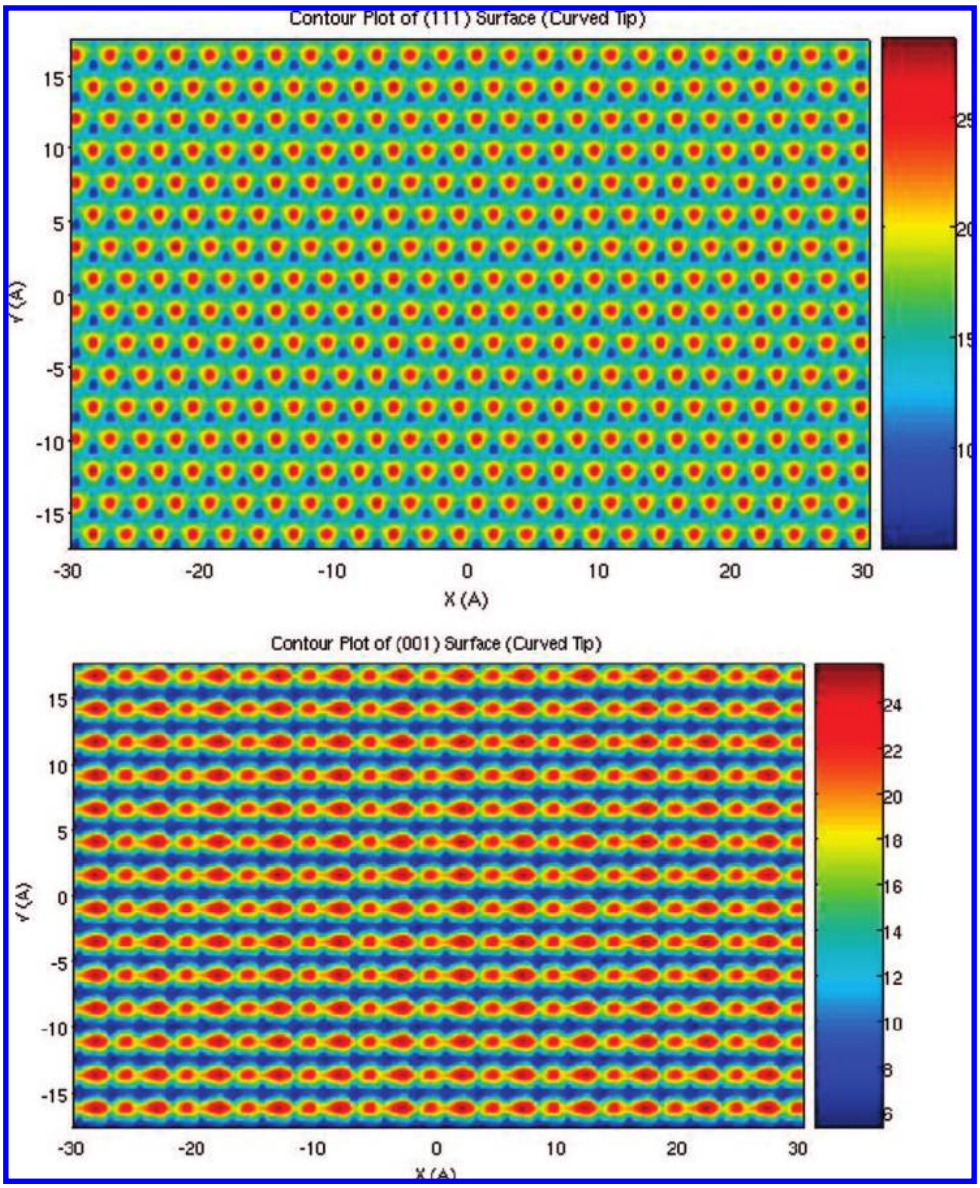

Figure 9. Potential energy landscape between the curved tip and the diamond (111) and (001) surfaces are shown in the upper and lower panels, respectively. In the upper panel, x and y correspond to the $[1\bar{1}0]$ and $[11\bar{2}]$ directions, respectively. In the lower panel, x and y correspond to the [110] and $[1\bar{1}0]$ directions, respectively. The color bar gives the energy between tip and surface in electronvolts. Areas with the highest energy (red) correspond to positions of surface hydrogen atoms.

that, in certain cases, the disagreement between simulation and continuum theory can be significant.[18,63,64] Continuum mechanics may substantially underestimate the area of contact for nanoscale, single-asperity contacts. However, while the quantitative values that emerge from continuum fits to AFM data may be suspect, a comparison of values obtained under the same experimental conditions certainly remains valid and is widely used.

In addition to the quantities actually measured in the AFM experiment, such as pull-off force (adhesion), the COS fits to the AFM data allow for the calculation of γ, $\tilde{C}$, the friction at zero load, and τ_0. The values of these quantities reported herein compare favorably to previously published values for similar interfaces. For example, two hydrogen-terminated hydrocarbon tips, of different radii, were used recently to examine the adhesion and friction of diamond (111)(1 × 1)-H and (001)(2 × 1)-H surfaces in dry N_2 at 300 K.[18] The range of reported values for the pull-off (adhesion) forces (25−54 nN), the work of adhesion values (36−200 mJ/m^2), and the friction at zero load (5.0−11.4 nN) is similar to the values reported here for a

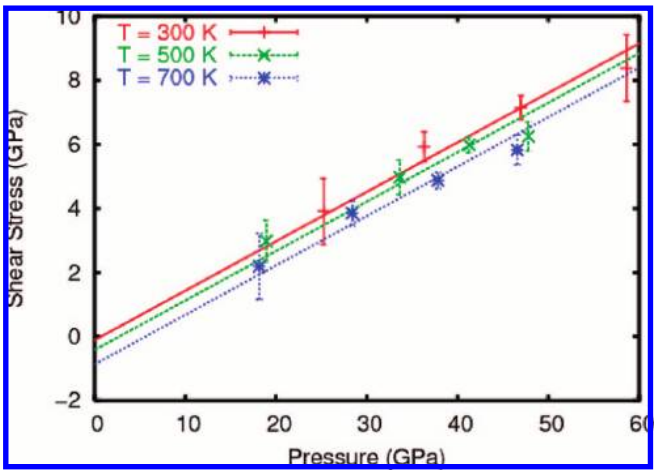

Figure 10. Shear stress (kinetic friction/contact area) as a function of normal pressure (normal force/contact area) calculated from MD simulations. These data were calculated while sliding in the $[1\bar{1}0]$ direction on the diamond (111) surface.

μCD−single-crystal diamond interface at the highest temperature. While general agreement in the magnitude of the numbers is quite good, there are some noteworthy differences between the values reported here and the published values for similar interfaces. These differences are discussed below.

In this work, the larger tip typically yielded larger values of the pull-off force, which is consistent with the idea that larger contact areas are obtained with larger tips. In contrast, this trend was not apparent in the pull-off forces between two amorphous hydrocarbon tips ($R = 45$ and 150 nm) and diamond (111)(1 × 1)-H or (001)(2 × 1)-H. In that work, particular care was taken to ensure that both the tips and the surfaces were completely hydrogen-terminated. As a result, the values of the pull-off forces obtained with both tips were nearly indistinguishable. Complete agreement between that study and this work should not be expected in view of the fact that the diamond surfaces in this study, and probably the diamond tips, contained a small amount of surface oxygen.

For diamond(111)(1 × 1)-H in UHV at 300 K, a previous AFM study that utilized a tungsten−carbide tip ($R = 110$ nm) measured a work of adhesion of ∼10 mJ/m^2.[17] When two amorphous hydrocarbon tips ($R = 45$ and 150 nm) were used to obtain γ values of diamond (111)(1 × 1)-H and (001)(2 × 1)-H at 300 K, the larger tip consistently yielded smaller values of γ.[18] When the small (large) tip was used, γ was ∼100 mJ/m^2 (∼36 mJ/m^2) on the (111) surface and ∼250 mJ/m^2 (∼64 mJ/m^2) on the (001) surface. In this work, the values of γ at 225 K are comparable to the values obtained with both the larger hydrocarbon tip[18] and those obtained with the tungsten−carbide tip.[17]

The values of γ reported here are similar for both surfaces at 225 K with the exception of γ for the (111) surface obtained using tip-2. In fact, values of γ obtained with tip-2 on (111) are consistently larger at all temperatures than the values measured with tip-1 or the values for the (001) surface measured with tip-2. There are a number of factors that could contribute to the range of values obtained for the work of adhesion. While both of the tips used here were commercial μCD tips, there could be differences in their surface chemistry. Small differences in the surface chemistry in different regions of a sample can cause values obtained from AFM measurements to vary with changing location on the sample. In addition, there was some evidence of wear for tip-2. On multiple occasions, adhesion forces increased with successive measurements at a given temperature, suggesting that tip-2 became progressively blunter with time. After completion of the measurements, tip-2 had a significantly larger end radius than tip-1, which did not exhibit this behavior. Finally, simulations have shown that relative orientation of the tip and sample and surface roughness impact γ with commensurate contacts having γ values that are approximately a factor of 2 larger.[64]

Recent ab initio calculations of the absolute surface energies per unit area of diamond found the unreconstructed (001)-H surface to have a lower surface energy than (111)-H by nearly 1 J/m^2.[42] The (001)(2 × 1)-H surface was not considered in that study, but it should have an even lower surface energy than the unreconstructed case. The values of γ obtained with tip-2 are in agreement with this study. However, the same trend was not obtained with tip-1 nor in the previous AFM study.[18] What these studies make clear is that additional verification of the work of adhesion values is needed on each diamond surface and that variables such as surface contamination, tip−sample orientation, roughness, measurement location, environment, and temperature must be highly controlled. In the data presented here, the friction force at zero load is larger when the larger tip was used at all the temperatures examined. This trend also was observed in the measurements of the friction between amorphous carbon tip and hydrogen-terminated diamond crystallites.[18]

The COS fits to the AFM data revealed that the friction versus load data reported here can be fit by the DMT contact model at all temperatures. This is not surprising in view of the fact that previous AFM measurements in UHV have shown that the current between the tip and the sample as a function of load for a hard heterocontact (i.e., a tungsten−carbide tip and diamond (111)(1 × 1)-H) can be described by DMT contact mechanics.[17,20] In addition, because the actual contact area was calculated from the tip−sample current, the friction force was shown to be a linear function of the contact area ($F_f = \tau_0 A$).[20] The value of interfacial shear strength for the tungsten−carbide diamond (111)(1 × 1)-H interface at room temperature in UHV was determined to be 238 MPa. This value of τ_0 compares well with the values reported here at 225 K for the μCD−single-crystal diamond interface.

While the values of τ_0 obtained with each μCD tip differ slightly, it is encouraging that the range of τ_0 values obtained with each tip is close to the value reported for the tungsten−carbide diamond interface and that both tips reproduce the same general trend in τ_0 with temperature. The shear strength of the interface should not exceed the ideal shear strength of the tip or sample. The ideal shear strength can be estimated to be $\approx G/30$, where G is the shear modulus of the tip or sample. The values of the ideal shear strength calculated using the values of $G_{(001)}$ and $G_{(111)}$ reported previously[18] are 19 and 17 GPa for the (001)(2 × 1)-H and the (111)(1 × 1)-H surfaces, respectively. These values are well above the range of values obtained for τ_0 reported here.

In the AFM experiments, the magnitude of the measured friction force is impacted by tip−sample adhesion. The experiments reported here were performed in the limit of negligible wear, and the data were analyzed so that the effects due to adhesion could be largely separated from properties such as interfacial shear strength. MD simulations also were performed in the wearless regime and in the absence of long-range adhesive forces between tip and sample. Although the size of the error bars in the simulations makes drawing unambiguous conclusions difficult, the average friction force obtained at a given temperature decreases slightly with increasing temperature on both surfaces for the two values of applied load examined. The values of the interfacial shear strength, τ_0, from the AFM measurements also decrease slightly with increasing temperature. The MD simulations provide additional insight into these findings. Previous MD simulations that examined the friction between two, infinitely flat, hydrogen-terminated diamond surfaces have shown that as hydrogen atoms on opposing surfaces come into close proximity, the friction force increases. Once a critical force is achieved, the hydrogen atoms slip past each other by bending or rotating out of each other's way. This process is aided by the additional vibrational motion of the atoms that is provided when the temperature is increased.[71]

Recently, MD simulations examined the effects of adsorbed layers on static and kinetic friction.[69,70] These studies show that the shear stress τ_s rises linearly with the local pressure P and can be explained using a simple hard-sphere picture. Briefly, two surfaces in close proximity create a surface of closest approach, in which the sliding surface must climb up to move laterally. The lateral force and normal force are related by the local slope of this surface, and α represents some average of the slope. As a result, parameters, such as temperature, pressure,

and surface−surface coupling energy, that do not influence the hard-sphere diameter have little effect on this slope and, thus, on α. In contrast, changes in nearest-neighbor spacing (i.e., geometry of the contact) change α dramatically.[69] For the static and kinetic friction between the curved-diamond tip and the (111) surface reported here, the value of α also is insensitive to temperature. The sliding direction affects the local slope of the contacting surfaces and thus explains the observed correlation in the MD friction $F_{[1\bar{1}0]}(111) > F_{[\bar{1}10]}(001)$ with surface atom density $\sigma_{(111)} > \sigma_{(001)}$. The quantity τ_a has been shown to decrease with increasing temperature because it decreases entropic repulsion.[69] This effect also was observed in this work.

While the dependence of the friction on temperature has not been previously measured between μCD tip and single-crystal diamond substrates in UHV with AFM, measurements between a silicon oxide tip and Si (111) wafer with the native oxide layer[22] and a Si_3N_4 tip and graphite[23] both in UHV were recently published. For the silicon tip and (111) wafer,[22] the pull-off force as a function of temperature and the friction force as a function of load at various temperatures were both reported. In that work, two different tips were used, and the pull-off force obtained with both tips increased from 55 to 100 K and then decreased between 100 and 300 K. In the work presented here, with the exception of tip-2 on the (001) surface, the pull-off force decreased slightly as the temperature increased. In the case of the Si_3N_4 tip on HOPG,[23] the pull-off force oscillated slightly between 800 and below 150 K and then showed a marked drop at 150 K. The surface chemistry, orientation, and surface roughness of the contacting pairs in each experiment are, undoubtedly, different; thus, agreement among the experiments cannot necessarily be expected.

Gnecco et al. examined the velocity dependence of sliding friction between the tip of a friction force microscope and a NaCl (100) surface. The lateral force was found to depend logarithmically on the velocity at a fixed temperature.[72] The experimental results were interpreted using a Tomlinson model modified to take into account thermal activation.[73] In this model, the interaction of the friction force microscope with the surface is described by a potential with a periodic term for the tip−surface interactions and a second term for the elastic energy stored in the cantilever. At zero temperature, the tip slips to a new minimum when the energy barrier between adjacent minima of the potential vanishes. At finite temperatures, the probability of a slip event must be examined. The maximum transition probability occurs at an extremum of the probability as a function of lateral force. Evaluation of the maximum transition probability yielded an expression for the lateral force as a function of velocity that was consistent with the experimentally determined data.

Sang et al. recently modeled the friction measured by an AFM tip as it is dragged across a surface at finite temperatures.[74] In addition, their numerical data were shown to be well-described by the thermal activation model.[72] Numerical simulations were performed that examined the average friction force for a range of scanning velocities (5 nm/s to 256 μm/s) and temperatures (53−373 K). Two distinct regimes were apparent in the dependence of the average friction force on temperature. For velocities greater than 22 μm/s, the average friction force was independent of temperature at fixed velocities. In contrast, for speeds down to 5 nm/s, increasing the temperature resulted in a small decrease in the average friction force with the effect becoming slightly larger as the speed was lowered. In fact, plots of average friction force versus temperature at fixed velocities are linear with the slope increasing in magnitude as the velocity decreases.

Both AFM and MD data presented here show a mild decrease in interfacial shear strength and average friction force with the AFM data providing experimental verification of the thermal activation model. In terms of a thermal activation model, the maximum in the distribution of forces that can result in a slip to an adjacent minimum is shifted to slightly lower values of force as the temperature increases.[75] Thus, the shear strength of the interface should gently decrease with increasing temperature. The qualitative explanation for the reduction in friction with increasing temperature gleaned from the MD simulations also agrees with the thermal activation model. The additional thermal motion associated with the additional temperature reduces the force where the tip slides just as the maximum in the distribution of the forces is shifted with decreasing temperature.

In this work, friction versus load data obtained with AFM possessed a nonlinearity that has been observed for many single-asperity contacts. There are also cases where linear friction versus load data were obtained using AFM.[22,23,76] The nonlinear behavior of the friction versus load data should be most apparent at negative values of applied load. When the temperature dependence of friction of silicon was examined, the friction at negative load values was not reported, so the existence of any nonlinearity could not be ascertained.[22] The dependence of friction on load has been studied extensively using analytical models and MD simulations. Extensive MD simulations showed that many different effects can lead to deviations between atomistic behavior and continuum theory. The tip geometry or structure has the most pronounced effect on friction and lateral stiffness because these quantities depend on the interlocking of atoms at the interface. The friction of nonadhesive commensurate tips increases linearly with load, while in other cases, such as amorphous tips, friction is a nonlinear function of load.[63,64] Linear friction−load relations were produced by MD simulations presented here. While this tip is not commensurate with both diamond surfaces, clearly it is more ordered than disordered. Thus, the linear behavior of the friction with load makes sense. It should be noted, however, that the origins of linear versus nonlinear friction load behavior, the connection with contact area, and the breakdown of continuum mechanics requires further experimental and theoretical examination.

Conclusion

The μCD−single-crystal diamond interface was examined experimentally by AFM in UHV and theoretically by MD as a function of temperature. Across a range of crystalline orientations and sliding directions, the experiments revealed that the pull-off force, the work of adhesion, and the interfacial shear strength decrease slightly with increasing temperature. The values of the interfacial shear strength, pull-off force, and work of adhesion are comparable to values obtained for similar interfaces at room temperature. The MD simulations reveal that the average friction force decreases slightly with increasing temperature for both diamond surfaces in all sliding directions. Insight into the mechanism by which friction is reduced with increasing temperature also is provided by MD simulations. Both AFM and MD data presented here are consistent with the previously published thermal activation model for tip-jumps at finite temperatures. The AFM data presented here provide experimental support for this model.

Acknowledgment. G.G. and M.J.B. acknowledge support from AFOSR as part of the Extreme Friction MURI (Contracts F1ATA08018G001 and F1ATA053001G004). J.A.H. acknowledges support from the ONR and AFOSR under Contracts N0001408WR20106 and F1ATA07351G001, respectively. M.J.B. and J.A.H. thank M. T. Knippenberg, J. D. Schall, R. J. Cannara, R. W. Carpick, K. J. Wahl, and M. O. Robbins for helpful discussions.

References and Notes

(1) Field, J. E. *The Properties of Diamond*; Academic Press: San Diego, 1979; pp 281−324.

(2) Field, J. E. *The Properties of Natural and Synthetic Diamond*; Academic Press: San Diego, 1992.

(3) Donnet, C.; Grill, A. Friction control of diamond-like carbon coatings. *Surf. Coat. Technol.* **1997**, *9*, 4–95, and 456−462.

(4) Erdemir, A.; Donnet, C. Tribology of diamond, diamond-like carbon, and related films. In *Modern Tribology Handbook*; Bhushan, B., Ed.; CRC Press LLC: Boca Raton, FL, 2001; Vol. 2, pp 871−908.

(5) Auciello, O.; Birrell, J.; Carlisle, J. A.; Gerbi, J. E.; Xiao, X. C.; Peng, B.; Espinosa, H. D. Materials science and fabrication processes for a new MEMS technology based on ultrananocrystalline diamond thin films. *J. Phys. C: Solid State Phys.* **2004**, *16*, 539–552.

(6) Gardos, M. N. Advantages and limitations of silicon as a bearing material for MEMS applications. In *Tribology Issues and Opportunities in MEMS*; Bhushan, B., Ed.; Kluwer Academic Publishers: Dordrecht, The Netherlands, 1998; pp 341−366.

(7) Kohn, E.; Ebert, W.; Adamschik, M.; Schmid, P.; Denisenko, A. Diamond-based MEMS devices. *New Diamond Frontier Carbon Technol.* **2001**, *11*, 81–100.

(8) Kohn, E.; Gluche, P.; Adamschik, M. Diamond MEMS−A New Emerging Technology. *Diamond Relat. Mater.* **1999**, *8*, 934–940.

(9) Sekaric, L.; Parpia, J. M.; Craighead, H. G.; Feygelson, T.; Houston, B. H.; Butler, J. E. Nanomechanical resonant structures in nanocrystalline diamond. *Appl. Phys. Lett.* **2002**, *81*, 4455–4457.

(10) Hayward, I. P. Friction and wear properties of diamond and diamond coatings. *Surf. Coat. Technol.* **1991**, *49*, 554–559.

(11) Field, J. E.; Pickles, C. S. J. Strength, fracture, and friction properties of diamond. *Diamond Relat. Mater.* **1996**, *5*, 625–634.

(12) Enomoto, Y.; Tabor, D. The frictional anisotropy of diamond. *Proc. R. Soc. London, Ser. A* **1981**, *373*, 405–417.

(13) Grillo, S. E.; Field, J. E. The friction of natural and CVD diamond. *Wear* **2003**, *254*, 945–949.

(14) Feng, Z.; Field, J. E. *J. Phys. D: Appl. Phys.* **1992**, *25*, 33–37.

(15) Germann, G. J.; Cohen, S. R.; Neubauer, G.; McClelland, G. M.; Seki, H.; Coulman, D. Atomic scale friction of a diamond tip on diamond (100)-surface and (111)-surface. *J. Appl. Phys.* **1993**, *73*, 163–167.

(16) Schwarz, U. D.; Zworner, O.; Koster, P.; Wiesendanger, R. Quantitative analysis of the frictional properties of solid materials at low loads. 0.1. Carbon compounds. *Phys. Rev. B: Condens. Matter Mater. Phys.* **1997**, *56*, 6987–6996.

(17) Enachescu, M.; van den Oetelaar, R. J. A.; Carpick, R. W.; Ogletree, D. F.; Flipse, C. F. J.; Salmeron, M. Atomic force microscopy study of an ideally hard contact: The diamond(111) tungsten carbide interface. *Phys. Rev. Lett.* **1998**, *81*, 1877–1880.

(18) Gao, G. T.; Cannara, R. J.; Carpick, R. W.; Harrison, J. A. Atomic-scale friction on diamond: A comparison of different sliding directions on (001) and (111) surfaces using MD and AFM. *Langmuir* **2007**, *23* (10), 5394–5405.

(19) van den Oetelaar, R. J. A.; Flipse, C. F. J. Atomic-scale friction on diamond(111) studied by ultra-high vacuum atomic force microscopy. *Surf. Sci.* **1997**, *384*, L828–L835.

(20) Enachescu, M.; van den Oetelaar, R. J. A.; Carpick, R. W.; Ogletree, D. F.; Flipse, C. F. J.; Salmeron, M. Observation of proportionality between friction and contact area at the nanometer scale. *Tribol. Lett.* **1999**, *7*, 73–78.

(21) Derjaguin, B. V.; Muller, V. M.; Toporov, Y. P. Effect of contact deformations on adhesion of particles. *J. Colloid Interface Sci.* **1975**, *53*, 314–326.

(22) Schirmeisen, A.; Jansen, L.; Holscher, H.; Fuchs, H. Temperature dependence of point contact friction on silicon. *Appl. Phys. Lett.* **2006**, *88*, (023108), 1–3.

(23) Zhao, X. Y.; Hamilton, M.; Sawyer, W. G.; Perry, S. S. Thermally activated friction. *Tribol. Lett.* **2007**, *27* (1), 113–117.

(24) Burris, D. L.; Perry, S. S.; Sawyer, W. G. Macroscopic evidence of thermally activated friction with polytetrafluoroethylene. *Tribol. Lett.* **2007**, *27* (3), 323–328.

(25) Burton, J. C.; Taborek, P.; Rutledge, J. E. Temperature dependence of friction under cryogenic conditions in vacuum. *Tribol. Lett.* **2006**, *23* (2), 131–137.

(26) Bhushan, B.; Israelachvili, J. N.; Landman, U. Nanotribology—Friction, wear, and lubrication at the atomic scale. *Nature (London, U.K.)* **1995**, *374* (6523), 607–616.

(27) Gao, J. P.; Luedtke, W. D.; Gourdon, D.; Ruths, M.; Israelachvili, J. N.; Landman, U. Frictional forces and Amontons' law: From the molecular to the macroscopic scale. *J. Phys. Chem. B* **2004**, *108* (11), 3410–3425.

(28) Landman, U.; Luedtke, W. D.; Burnham, N. A.; Colton, R. J. Atomistic mechanisms and dynamics of adhesion, nanoindentation, and fracture. *Science (Washington, DC, U.S.)* **1990**, *248* (4954), 454–461.

(29) Meyer, G.; Amer, N. M. Simultaneous measurement of lateral and normal forces with an optical-beam-deflection atomic force microscope. *Appl. Phys. Lett.* **1990**, *57*, 2089–2091.

(30) Carpick, R. W.; Salmeron, M. Scratching the surface: Fundamental investigations of tribology with atomic force microscopy. *Chem. Rev.* **1997**, *97*, 1163–1194.

(31) Cannara, R. J.; Eglin, M.; Carpick, R. W. Lateral force calibration in atomic force microscopy: A new lateral force calibration method and general guidelines for optimization. *Rev. Sci. Instrum.* **2006**, *77*, (53701), 1–11.

(32) Ogletree, D. F.; Carpick, R. W.; Salmeron, M. Calibration of frictional forces in atomic force microscopy. *Rev. Sci. Instrum.* **1996**, *67*, 3298–3306.

(33) Sader, J. E.; Chon, J. W. M.; Mulvaney, P. Calibration of rectangular atomic force microscope cantilevers. *Rev. Sci. Instrum.* **1999**, *70* (10), 3967–3969.

(34) Carpick, R. W.; Ogletree, D. F.; Salmeron, M. A general equation for fitting contact area and friction versus load measurements. *J. Colloid Interface Sci.* **1999**, *211*, 395.

(35) Cannara, R. J.; Brukman, M. J.; Carpick, R. W. Cantilever tilt compensation for variable-load atomic force microscopy. *Rev. Sci. Instrum.* **2005**, *76*, (53706), 1–6.

(36) Brukman, M. J.; Marco, G. O.; Dunbar, T. D.; Boardman, L. D.; Carpick, R. W. Nanotribological properties of alkanephosphonic acid self-assembled monolayers on aluminum oxide: Effects of fluorination and substrate crystallinity. *Langmuir* **2006**, *22* (9), 3988–3998.

(37) Yang, H. X.; Xu, L. F.; Gu, C. Z.; Zhang, S. B. First-principles study of oxygenated diamond (001) surfaces with and without hydrogen. *Appl. Surf. Sci.* **2007**, *253* (9), 4260–4266.

(38) Berendsen, H. J. C.; Postma, J. P. M.; van Gunsteren, W. F.; DiNola, A.; Haak, J. R. Molecular dynamics with coupling to an external bath. *J. Chem. Phys.* **1984**, *81*, 3684–3690.

(39) Brenner, D. W.; Shenderova, O. A.; Harrison, J. A.; Stuart, S. J.; Ni, B.; Sinnott, S. B. Second generation reactive empirical bond order (REBO) potential energy expression for hydrocarbons. *J. Phys. C: Solid State Phys.* **2002**, *14*, 783–802.

(40) Brenner, D. W. The art and science of an analytic potential. *Phys. Status Solidi B* **2000**, *217* (1), 23–40.

(41) Brenner, D. W. Empirical potential for hydrocarbons for use in simulating chemical vapor deposition of diamond films. *Phys. Rev. B: Condens. Matter Mater. Phys.* **1990**, *42*, 9458–9471.

(42) Stekolnikov, A. A.; Furthmüller, J.; Bechstedt, F. Absolute surface energies of group-IV semiconductors: Dependence on orientation and reconstruction. *Phys. Rev. B: Condens. Matter Mater. Phys.* **2002**, 65 (115318), 1–10.

(43) Yakobson, B. I.; Brabec, C. J.; Bernholc, J. Nanomechanics of carbon tubes: Instabilities beyond linear response. *Phys. Rev. Lett.* **1996**, *76*, 2511–2514.

(44) Brenner, D. W.; Dunlap, B. I.; Harrison, J. A.; Mintmire, J. W.; Mowrey, R. C.; Robertson, D. H.; White, C. T. Group IV covalent clusters: Si45 and C44 versus Si44 and C45. *Phys. Rev. B: Condens. Matter Mater. Phys.* **1991**, *44*, 3479–3482.

(45) Harrison, J. A.; Brenner, D. W.; White, C. T.; Colton, R. J. Atomistic mechanisms of adhesion and compression of diamond surfaces. *Thin Solid Films* **1991**, *206* (1−2), 213–219.

(46) Harrison, J. A.; White, C. T.; Colton, R. J.; Brenner, D. W. Nanoscale investigation of indentation, adhesion, and fracture of diamond (111) surfaces. *Surf. Sci.* **1992**, *271* (1−2), 57–67.

(47) Perry, M. D.; Harrison, J. A. Universal aspects of the atomic-scale friction of diamond surfaces. *J. Phys. Chem.* **1995**, *99*, 9960–9965.

(48) Harrison, J. A.; Brenner, D. W. Simulated tribochemistry: An atomic-scale view of the wear of diamond. *J. Am. Chem. Soc.* **1994**, *116*, 10399–10402.

(49) Harrison, J. A.; White, C. T.; Colton, R. J.; Brenner, D. W. Effects of chemically bound, flexible hydrocarbon species on the frictional properties of diamond surfaces. *J. Phys. Chem.* **1993**, *97*, 6573–6576.

(50) Gao, G. T.; Mikulski, P. T.; Chateauneuf, G. M.; Harrison, J. A. The effects of film structure and surface hydrogen on the properties of amorphous carbon films. *J. Phys. Chem. B* **2003**, *107*, 11082–11090.

(51) Gao, G. T.; Mikulski, P. T.; Harrison, J. A. Molecular-scale tribology of amorphous carbon coatings: Effects of film thickness, adhesion, and long-range interactions. *J. Am. Chem. Soc.* **2002**, *124*, 7202–7209.

(52) Shenderova, O. A.; Brenner, D. W. Atomistic simulations of structures and mechanical properties of <011> tilt grain boundaries and

their triple junctions in diamond. *Phys. Rev. B: Condens. Matter Mater. Phys.* **1999**, *60* (10), 7053–7061.

(53) Shenderova, O. A.; Brenner, D. W. Atomistic simulation of grain boundaries, triple junctions, and related disclinations. *Solid State Phenom.* **2002**, *87*, 205–213.

(54) Gao, G. T.; Van Workum, K.; Schall, J. D.; Harrison, J. A. Elastic constants of diamond from molecular dynamics simulations. *J. Phys.: Condens. Matter* **2006**, *18*, S1737–S1750.

(55) Van Workum, K.; Gao, G. T.; Schall, J. D.; Harrison, J. A. Expressions for the stress and elasticity tensors for the angle-dependent potentials. *J. Chem. Phys.* **2006**, 125 (144506), 1–10.

(56) Stuart, S. J.; Tutein, A. B.; Harrison, J. A. A reactive potential for hydrocarbons with intermolecular interactions. *J. Chem. Phys.* **2000**, *112*, 6472–6486.

(57) Harrison, J. A.; Schall, J. D.; Knippenberg, M. T.; Gao, G.; Mikulski, P. T. Elucidating Atomic-Scale Friction using Molecular Dynamics and Specialized Analysis Techniques *J. Phys.: Condens. Matter* **2008**, in press

(58) Johnson, K. L.; Kendall, K.; Roberts, A. D. Surface energy and contact of elastic solids. *Proc. R. Soc. London, Ser. A* **1971**, *324*, 301–313.

(59) Maugis, D. Adhesion of spheres−The JKR-DMT transition using a Dugdale model. *J. Colloid Interface Sci.* **1992**, *150*, 243–269.

(60) Schwarz, U. D. A generalized analytical model for the elastic deformation of an adhesive contact between a sphere and a flat surface. *J. Colloid Interface Sci.* **2003**, *261* (1), 99–106.

(61) Carpick, R. W.; Agrait, N.; Ogletree, D. F.; Salmeron, M. Variation of the interfacial shear strength and adhesion of a nanometer-sized contact. *Langmuir* **1996**, *12*, 3334–3340.

(62) Grierson, D. S.; Flater, E. E.; Carpick, R. W. Accounting for the JKR-DMT transition in adhesion and friction measurements with atomic force microscopy. *J. Adhesion Sci. Technol.* **2005**, *19*, 291–311.

(63) Luan, B. Q.; Robbins, M. O. The breakdown of continuum models for mechanical contacts. *Nature (London, U.K.)* **2005**, *435*, 929–932.

(64) Luan, B. Q.; Robbins, M. O.; Contact of single asperities with varying adhesion: Comparing continuum mechanics to atomistic simuations*Phys. Rev. E: Stat., Nonlinear, Soft Matter Phys.* **2006**, *74*(26111),1–11.

(65) He, G.; Muser, M. H.; M.O., R. Adsorbed layers and the origin of static friction. *Science (Washington, DC, U.S.)* **1999**, *284*, 1650–1662.

(66) Turley, J.; Sines, G. The anisotropy of Young's Modulus, shear modulus, and Poisson's ratio in cubic materials. *J. Phys. D: Appl. Phys.* **1971**, *4*, 264–271.

(67) Zouboulis, E. S.; Grimsditch, M.; Ramdas, A. K.; Rodriguez, S. Temperature dependence of the elastic moduli of diamond: A Brillouin-scattering study. *Phys. Rev. B: Condens. Matter Mater. Phys.* **1998**, *57*, 2889–2896.

(68) Yates, B. *Thermal Expansion*; Plenum: New York, 1972.

(69) He, G.; Robbins, M. O.; Simulations of the static friction due to adsorbed molecules*Phys. Rev. B: Condens. Matter Mater. Phys.* **2001**, *3*(35413),1–13.

(70) He, G.; Robbins, M. O. Simulations of the kinetic friction due to adsorbed surface layers. *Tribol. Lett.* **2001**, *10* (1−2), 7–14.

(71) Harrison, J. A.; White, C. T.; Cotton, R. J.; Brenner, D. W. Molecular Dynamics Simulations of Atomic Scale Friction of Diamond Surfaces. *Phys. Rev. B.* **1992**, *46*, 9700–9708.

(72) Gnecco, E.; Bennewitz, R.; Gyalog, T.; Loppacher, C.; Bammerlin, M.; Meyer, E.; Guntherodt, H. J. Velocity dependence of atomic friction. *Phys. Rev. Lett.* **2000**, *84* (6), 1172–1175.

(73) Tomlinson, G. A. A molecular theory of friction. *Philos. Mag.* **1929**, *7* (46), 905–939.

(74) Sang, Y.; Dube, M.; Grant, M.; Thermal effects on atomic friction*Phys. Rev. Lett.* **2001**, *87*(174301),1–4.

(75) Schirmeisen, A.; Jansen, L.; Fuchs, H.; Tip-jump statistics of stick-slip friction*Phys. Rev. B: Condens. Matter Mater. Phys.* **2005**, *71*(245403),1–7.

(76) Mate, C. M. Nanotribology studies of carbon surfaces by force microscopy. *Wear* **1993**, *168*, 17–20.

JP711959E